Quantum criticality in the two-dimensional dissipative quantum XY model

Lijun Zhu, Changtao Hou, and Chandra M. Varma

Department of Physics and Astronomy, University of California, Riverside, California 92521, USA

(Received 26 May 2016; revised manuscript received 28 September 2016; published 28 December 2016)

Earlier Monte Carlo calculations on the dissipative two-dimensional XY model are extended in several directions. We study the phase diagram and the correlation functions when dissipation is very small, where it has properties of the classical 3D-XY transition, i.e., one with a dynamical critical exponent $z = 1$. The transition changes from $z = 1$ to the class of criticality with $z \to \infty$ driven by topological defects, discovered earlier, beyond a critical dissipation. We also find that the critical correlations have power-law singularities as a function of tuning the ratio of the kinetic energy to the potential energy for fixed large dissipation, as opposed to essential singularities on tuning dissipation keeping the former fixed. A phase with temporal disorder but spatial order of the Kosterlitz-Thouless form is also further investigated. We also present results for the transition when the allowed Caldeira-Leggett form of dissipation and the allowed form of dissipation coupling to the compact rotor variables are both included. The nature of the transition is then determined by the Caldeira-Leggett form.

I. INTRODUCTION

In a previous paper [1] (referred to as paper I), we have investigated the dissipative quantum XY (DQXY) model by quantum Monte Carlo calculations in two spatial dimensions (2D) for a range of parameters. This followed an earlier investigation of the same model [2]. The 2D dissipative quantum XY model has a number of applications. Originally proposed [3] in connection with superconductor to insulator transitions in thin metallic films [4], the same model describes the collective fluctuations in the planar itinerant fermion ferromagnet as well as the incommensurate Ising and the commensurate or incommensurate planar antiferromagnet [5,6]. It is also the model for the fluctuations of the loop-current ordered state [7] proposed and observed [8] in the underdoped region of the cuprates.

We had focused in paper I on the dissipation induced phase transitions in which the phase transition from the disordered state to the (2+1)D quantum ordered state occurs with the spatial correlation length ξ_r proportional to logarithm of the temporal correlation length ξ_τ. This may be said to imply a dynamical critical exponent $z \equiv d \ln \xi_\tau / d \ln \xi_r = \infty$. It is well understood that without dissipation, the model is Lorentz-invariant, so that $\xi_\tau \propto \xi_r$, i.e., $z = 1$. We present here the results of Monte Carlo calculations to investigate the phase diagram and correlation functions in an extended range of parameters to exhibit the transition of the dynamical critical exponents from $z = 1$ to $z = \infty$ as the dissipation is varied. We also investigate further the region of occurrence of a 2D spatial ordered region without temporal order, found in earlier Monte Carlo calculations [1,2]. We also discuss the question of the anisotropy of the correlation lengths in time and space in the nondissipative as well as the dissipative model, as well as the finite temperature crossover from a 2D Kosterlitz-Thouless type phase to (2+1)D order.

In paper I, the transition from the quantum disordered to the ordered phase was studied by varying the dissipation parameter α, and ξ_r and ξ_τ were calculated as a function of the deviation of the parameter α from its critical value. We complete the work in this region by calculating the correlation lengths near the transition by also varying the parameters for the kinetic energy and the potential energy in the model.

We find that the relation $\xi_r \propto \ln \xi_\tau$ is preserved, but that the dependence of ξ_τ on the deviation from critical value of these parameters is an algebraic singularity, rather than an essential singularity found for variation of α from its critical value. These calculations and results have important applications. While the (2+1)D superconductor-insulator transitions [4] are often tuned by varying dissipation through variation of disorder or film thickness, the transitions in metallic antiferromagnets are often tuned by varying pressure [9]. In that case, one expects that the transition is tuned by the variation of the ratio of the kinetic energy to the potential energy. Often, however, the transition in antiferromagnets as well as in the cuprates is tuned by doping. In that case, one expects both the dissipation and the ratio of the kinetic energy to the potential energy to be varied. Since the crossover from quantum-critical to quantum properties occurs as T changes from more than to less than $O(\xi_\tau^{-1})$, there should be a vastly wider region of quantum-critical properties for dissipation tuned transitions than for the transitions tuned by the ratio of the kinetic to the potential energy.

Several, but not all, of the Monte Carlo results have also been obtained in a recent analytical leading order renormalization group calculation [10] on a model of topological excitations derived from the starting dissipative quantum XY model. The transformation of the original model to that of topological excitations is possible only for finite dissipation. Therefore it has not been possible to get analytic results for the transition from the Lorentz-invariant $z = 1$ critical point to the $z \to \infty$ critical point at dissipation above a critical value. The present work provides such results.

We also note here the principal analytical works on the 2D-XY model without dissipation [3,11–13]. Our results in the dissipation free model are consistent with these works. We also obtain in our calculations, the rather obvious finite temperature crossover in that model to the Kosterlitz-Thouless quasiordered phase. The crossovers and the transitions in the dissipative model are new and interesting features and may have experimental relevance.

In paper I and most of the work here, we study the Caldeira-Leggett [14] form of dissipation. In this dissipation, the variable θ is unbounded. An alternate form of dissipation

is for θ to be a compact variable. In that case, one suspects from Monte Carlo calculations on a related model [15] that the critical fluctuations remain in the $z = 1$ class, i.e., of the same form as without dissipation. We investigate here and find this to be true in the quantum-XY model. Since, both forms of dissipation are allowed for the physical problems of interest, a worthwhile investigation is to study the transition when both forms of dissipation are allowed. We present some results here. We find that over a wide range of the compact dissipation parameter, the transition driven by the Caldeira-Leggett dissipation remains unaffected, i.e., it is of the $z \to \infty$ class.

II. THE MODEL

(2+1)D Quantum dissipative XY model

We investigate the action S of the 2D-DQXY model for the angle $\theta(\mathbf{x}, \tau)$ of fixed-length quantum rotors at space-imaginary time point $(\mathbf{x}, \tau)$:

$$
\begin{aligned}
S = &-K_0 \sum_{\langle \mathbf{x}, \mathbf{x}' \rangle} \int_0^\beta d\tau \cos(\theta_{\mathbf{x}, \tau} - \theta_{\mathbf{x}', \tau}) \\
&+ \frac{1}{2E_c} \sum_{\mathbf{x}} \int_0^\beta d\tau \left(\frac{d\theta_{\mathbf{x}}}{d\tau} \right)^2 + \frac{\alpha}{4\pi^2} \sum_{\langle \mathbf{x}, \mathbf{x}' \rangle} \int d\tau d\tau' \\
&\times \frac{\pi^2}{\beta^2} \frac{[(\theta_{\mathbf{x}, \tau} - \theta_{\mathbf{x}', \tau}) - (\theta_{\mathbf{x}, \tau'} - \theta_{\mathbf{x}', \tau'})]^2}{\sin^2 \left(\frac{\pi |\tau - \tau'|}{\beta} \right)} \\
&- h_4 \sum_{\mathbf{x}} \int d\tau \cos(4\theta_{\mathbf{x}, \tau}).
\end{aligned} \tag{1}
$$

τ is periodic in $[0, \beta]$, where $\beta = 1/(k_B T)$. $\langle \mathbf{x}, \mathbf{x}' \rangle$ denotes nearest neighbors. The first term is the spatial coupling term as in classical XY model. The second term is the kinetic energy where the charging energy E_c serves as the moment of inertia of the rotors. The third term describes quantum dissipations of the ohmic or Caldeira-Leggett type [14]. The last term describes effects of anisotropy on a lattice with four-fold anisotropy.

In the Monte Carlo calculations, a 2D square lattice with $N \times N$ sites is used. Periodic boundary conditions are imposed along both x and y directions. The imaginary time axis $[0, \beta]$ is split into N_τ slices. In the discretized (2+1)D lattice, the action can be written as [1,2]

$$
\begin{aligned}
S = &-K \sum_{\langle \mathbf{x}, \mathbf{x}' \rangle, \tau} \cos(\Delta\theta_{\mathbf{x}, \mathbf{x}', \tau}) + \frac{K_\tau}{2} \sum_{\mathbf{x}, \tau} (\theta_{\mathbf{x}, \tau} - \theta_{\mathbf{x}, \tau-1})^2 \\
&+ \frac{\alpha}{4\pi^2} \sum_{\langle \mathbf{x}, \mathbf{x}' \rangle, \tau, \tau'} \frac{\pi^2}{N_\tau^2} \frac{[\Delta\theta_{\mathbf{x}, \mathbf{x}', \tau} - \Delta\theta_{\mathbf{x}, \mathbf{x}', \tau'}]^2}{\sin^2 \left(\frac{\pi |\tau - \tau'|}{N_\tau} \right)},
\end{aligned} \tag{2}
$$

where $K_\tau \equiv 1/(E_c \Delta\tau)$, $K \equiv K_0 \Delta\tau$ are dimensionless kinetic energy and potential energy parameters. They have been normalized by the ultraviolet cutoff $\Delta\tau = \beta/N_\tau$. In this representation, the temperature is controlled by N_τ^{-1}. The calculations are asymptotically correct for the quantum problem where $1/\beta = T \to 0$ and $N_\tau \to \infty$, with their product held constant. This requires in practice that we

ensure that the results converge in the range of N_τ actually studied.

The fourfold lattice anisotropy h_4 is marginally irrelevant in the classical XY model [16], and irrelevant at the quantum transition [17,18], as verified in paper I. We have not included it in the calculation in this paper.

Quite obviously, a larger potential energy parameter K favors ordering and a larger kinetic energy parameter K_τ prefers a quantum-disordered state. In the absence of dissipation, i.e., for $\alpha = 0$, the transition to a 2+1 D ordered state at $T = 0$ therefore occurs for $1/(K K_\tau)$ below a critical value. In such a Lorentz invariant model, the ratio of the kinetic to the potential energy determines the effective velocity of the critical modes, and therefore also the ratio of the correlation length in time with respect to that in space. In interpreting the Monte Carlo results, it is useful to note that $1/(K K_\tau)$ is independent of T and N_τ. On the other hand, $K_\tau/K = (N_\tau T)^2/(K_0 E_c)$. Both the effects of the physical anisotropy parameter $K_0 E_c$, as well as information about finite temperature crossover due to the inevitable finite N_τ in the calculations are given by K_τ/K. These points are important to bear in mind when reading the phase diagrams deduced below.

The dimensionless dissipation parameter is defined as $\alpha = R_Q/R_s$, where R_s is the normal resistivity and $R_Q = h/4e^2$ is the quantum of resistivity. Please note that $\alpha/(4\pi^2)$ defined in this paper corresponds to α in Refs. [1,2]. We have made this change so that the critical point in the model as a function of dissipation occurs near the $\alpha = 1$ defined in this paper. Also, with this definition, the magnitude of α is easily interpreted physically.

A larger α (smaller normal state resistivity) promotes the ordered state. Since in two dimensions, strong localization occurs at low temperatures if the normal state resistance is of the order of the quantum of resistance, it can be argued that only models with $\alpha \gtrsim 0.2$ are relevant for applications to experiments for any of the metallic systems for which the present work may be applicable.

The procedure, accuracy, and limits of validity of the Monte Carlo calculations have all been given earlier in paper I in Sec. 2C. The same apply for the investigation here and need not be discussed again. In paper I, several physical quantities were defined to characterize the phases and the correlations. For convenience, they are defined again here.

Action susceptibility. The action susceptibility is defined as

$$
\chi_S = \frac{1}{N^2 N_\tau} (\langle S^2 \rangle - \langle S \rangle^2), \tag{3}
$$

where $\langle \ldots \rangle$ denotes averaging over the $O(10^6)$ Monte Carlo measurements. In classical systems, as $S = \beta H$, χ_S is related to the specific heat, $\chi_S = C_V/k_B$. At $T \to 0$, it is a measure of zero-point fluctuations which are expected to be singular at the critical point due to the degeneracy in the spectra.

Helicity modulus. The helicity modulus or spatial stiffness is defined as the change of energy due to a slow twist of spins
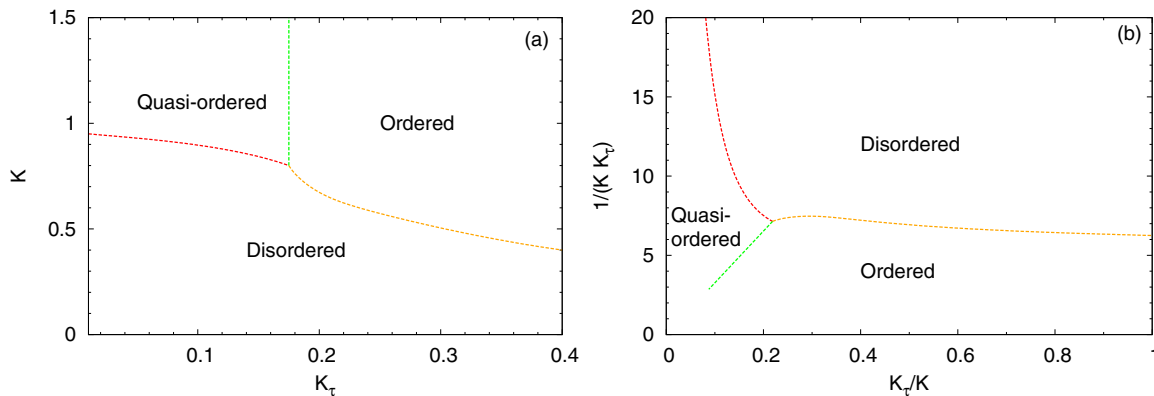
FIG. 1. (a) Phase diagram for $\alpha = 0$ in the K_τ-K plane and (b) the same in the (K_τ/K)-$1/(K_\tau K)$ plane. This phase diagram is constructed from calculations of various physical quantities in Figs. 2 and 3 for the values of K_τ and K for which the results are presented there. As explained in the text, $(K_\tau K)$ is independent of temperature, while $1/(K_\tau/K)$ depends on temperature as well as on the ultraviolet spatial and temporal scales in the Monte Carlo simulations. At $T \to 0$, the transition from the disordered to the Kosterlitz-Thouless type quasiordered phase as well as from the latter to the (2+1)D ordered phase occur as crossovers. The transition from the disordered to the ordered phase is of the 3D classical XY universality class. The implications of part (b) of the diagram for finite T crossovers and effects of temporal and spatial anisotropy are discussed in the text.

along the spatial direction, or

$$\Upsilon_x = \frac{1}{N^2 N_\tau} \left\langle \sum_{\langle \mathbf{x},\mathbf{x}' \rangle} \sum_\tau \cos(\Delta\theta_{\mathbf{x},\mathbf{x}',\tau}) \right\rangle$$
$$- \frac{K}{N^2 N_\tau} \left\langle \left(\sum_{\langle \mathbf{x},\mathbf{x}' \rangle} \sum_\tau \sin(\Delta\theta_{\mathbf{x},\mathbf{x}',\tau}) \right)^2 \right\rangle. \quad (4)$$

In the disordered state, the two terms have comparable contributions and $\Upsilon_x \to 0$. In an ordered phase, the second term vanishes, so that Υ_x is finite.
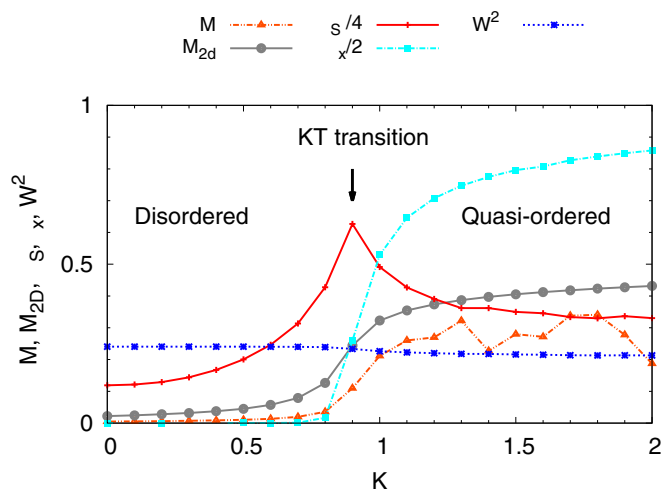

FIG. 2. Static properties defined in the text, for $\alpha = 0$, $K_\tau = 0.1$, and varying K over the 21 points shown. The results shown are for $N = 50$ and $N_\tau = 100$. A rapid growth and fall in χ_S denotes the passage across a symmetry breaking for a quantum transition. The rapid growth of the helicity modulus Υ_x and M and M_{2D}, as discussed in the text, reveal a finite size crossover from the disordered phase to quasiordered phase. The smooth behavior of W_θ^2 shows that temporal correlations do not change across this crossover, unlike the spatial correlations.

Order parameter. For XY model, the order parameter $\mathbf{M}(\mathbf{x},\tau) = (\cos\theta_{\mathbf{x},\tau}, \sin\theta_{\mathbf{x},\tau})$. Its modulus, the magnetization in the plane, is defined as

$$M = \frac{1}{N^2 N_\tau} \left\langle \left| \sum_{\mathbf{x},\tau} e^{i\theta_{\mathbf{x},\tau}} \right| \right\rangle. \quad (5)$$

In classical 2D XY model, the ordered phase has a quasilong-range order, where $M \sim (1/N)^{1/(8\pi K)}$, vanishes for $N \to \infty$. We also found it illuminating to calculate M_{2D}, the magnitude of magnetization in the planes at a given time τ and then average it over the τ. This is equivalent to finding the Kosterlitz-Thouless order parameter at each time slice and then averaging over the time slices.

$$M_{2D} = \frac{1}{N^2 N_\tau} \left\langle \sum_\tau \left| \sum_{\mathbf{x}} e^{i\theta_{\mathbf{x},\tau}} \right| \right\rangle. \quad (6)$$
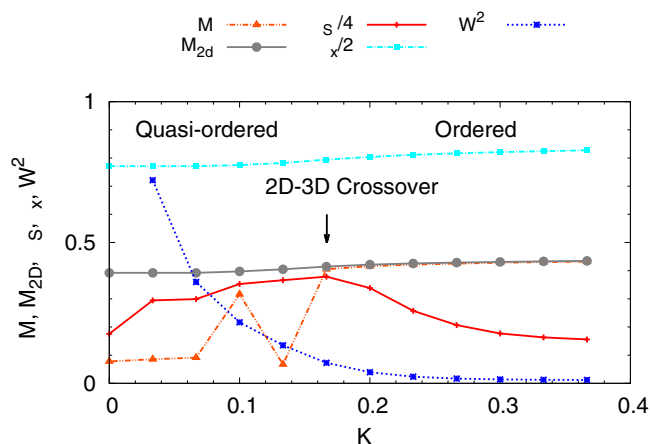

FIG. 3. Calculation of the specified static quantities showing results consistent with a transition (as $T \to 0$) from the quasiordered phase to the ordered phase for $\alpha = 0$, $K = 1.4$ by varying K_τ over the 12 different values shown. The rather large noise in the data is due to finite size effects discussed in the text.
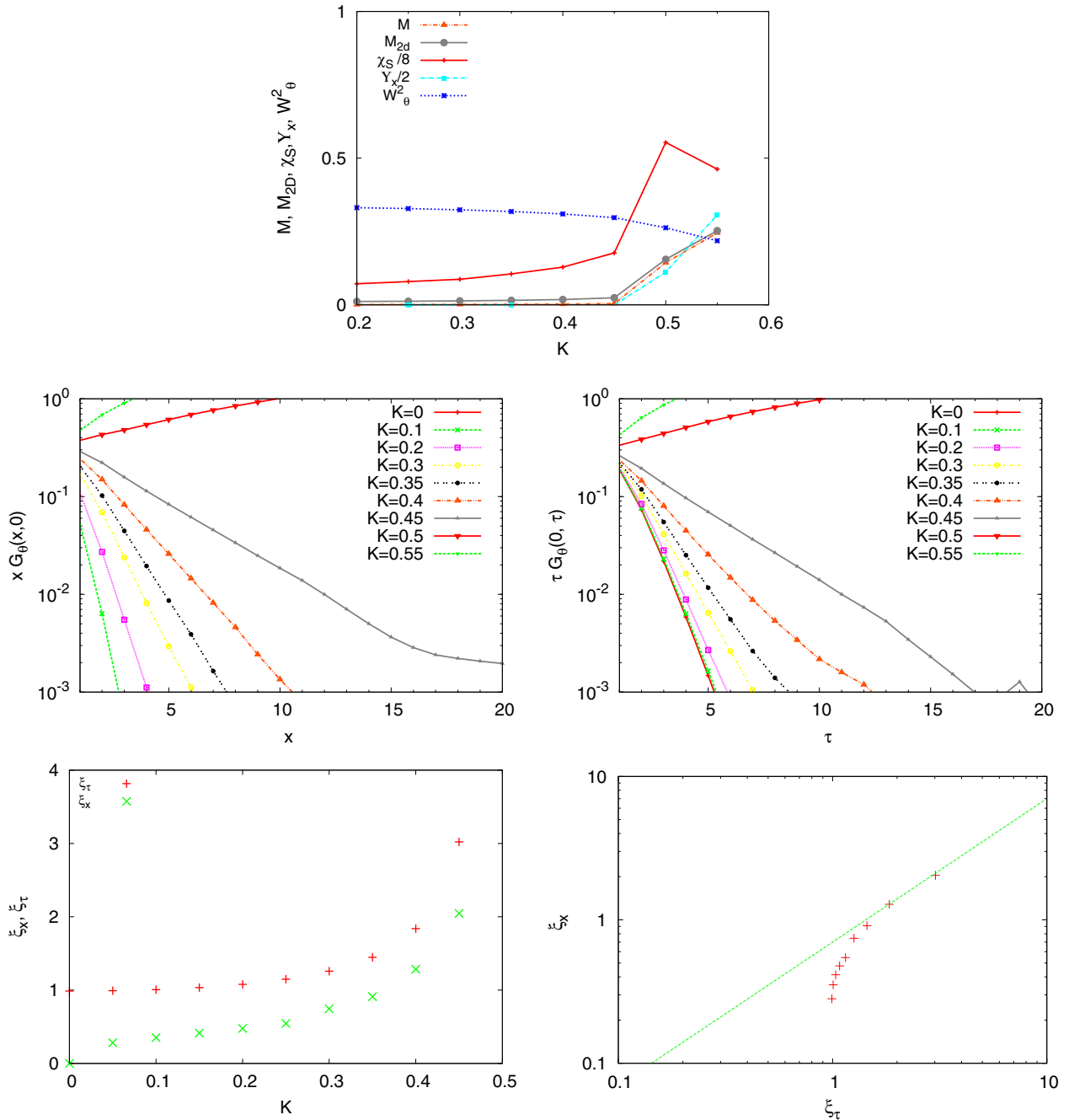
FIG. 4. A transition from disordered phase to ordered phase when $\alpha = 0$. Here, $K_\tau = 0.3$ and K is varied. The critical value for the potential energy parameter, K_c is between 0.45 and 0.5. In the first panel, static quantities are shown: M, M_{2D}, Υ_x achieve nonzero values across the transition. The next panels show the order parameter correlations, for fixed time as a function of x and for fixed x as a function of τ. We find $G_\theta(x,0) \sim (1/x) \exp(-x/\xi_x)$ and $G_\theta(0,\tau) \sim (1/\tau) \exp(-\tau/\xi_\tau)$. The final panels shows that close to the transition, the spatial correlation length $\xi_x \sim \xi_\tau$, the temporal correlation length for $\xi_x \gg 1$, i.e., the dynamical critical exponent $z \approx 1$, consistent with a 3D XY transition.

By definition $M \leq M_{2D}$. Also $M = M_{2D} \neq 0$ (for $N \to \infty$) only if there is perfect long-range order across time as well as space.

Local mean-square fluctuations of θ in time. We also calculate the spatially local mean-square fluctuations in $\theta(\tau)$, denoted by W_θ^2:

$$W_\theta^2 \equiv \frac{1}{N_\tau} \left\langle \sum_1^{N_\tau} (\Delta\theta_\tau - \overline{\Delta\theta})^2 \right\rangle. \tag{7}$$

Here, $\overline{\Delta\theta} = \frac{1}{N_\tau} \sum_1^{N_\tau} \Delta\theta_\tau$. As shown in Ref. [2] and in paper I, a rapid change in W_θ^2 is a measure of critical slowing down in transitions.

Correlation function of the order parameter. The principal results for the quantum-critical fluctuations are given by the order parameter correlation functions:

$$G_\theta(\mathbf{x},\tau) = \frac{1}{N^2 N_\tau} \sum_{\mathbf{x}',\tau'} \langle e^{i(\theta_{\mathbf{x}'+\mathbf{x},\tau'+\tau} - \theta_{\mathbf{x}',\tau'})} \rangle. \tag{8}$$
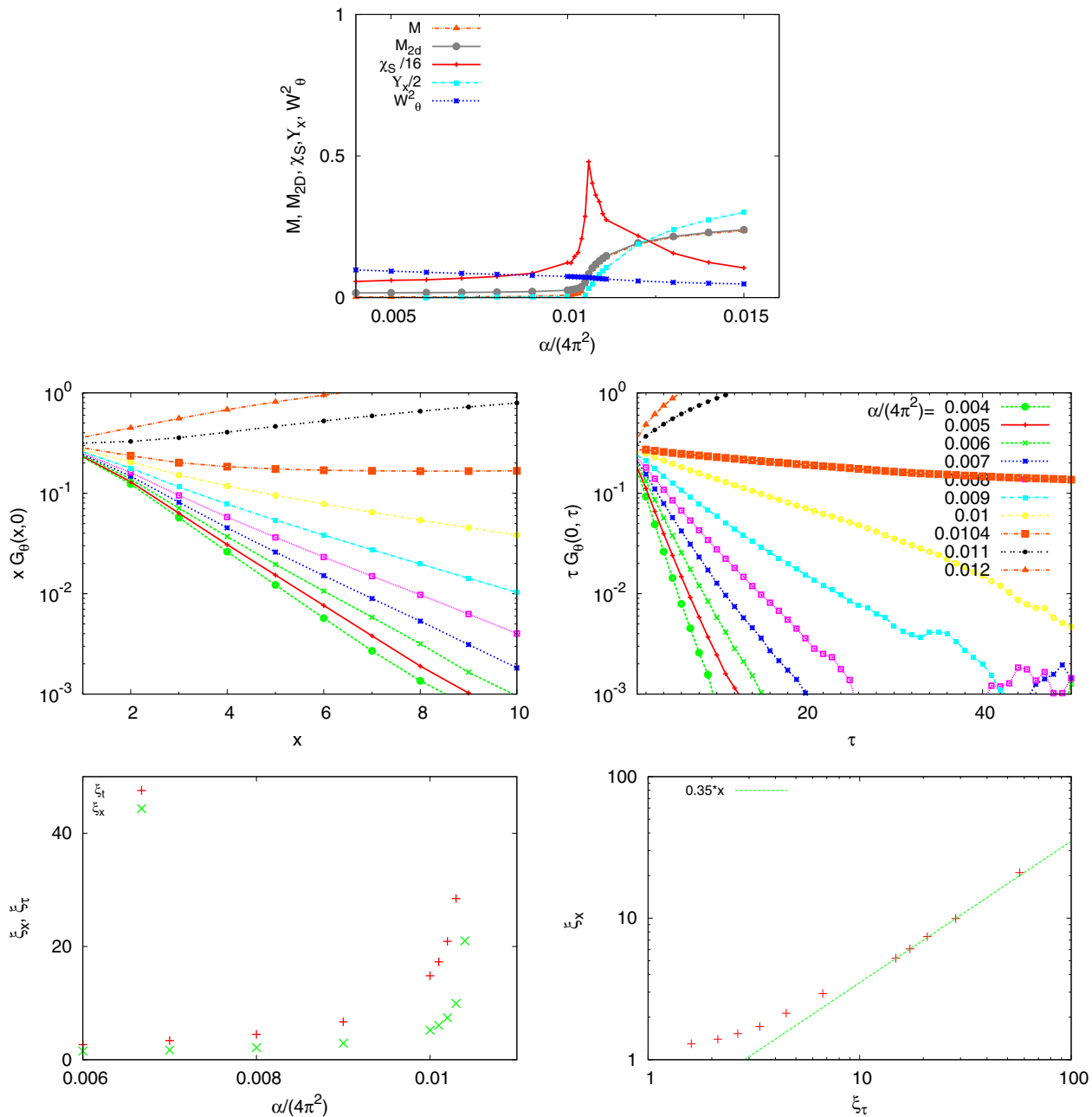
FIG. 5. This figure shows the same quantities as in Fig. 4 and in the same order but by varying α and for $K_\tau = 0.2$, $K = 0.4$. We find similar results as in the calculations for $\alpha = 0$ by varying K or K_τ. Most importantly, in the calculations shown in this and the preceding figure, $\xi_x \sim \xi_\tau$ near critical point, i.e., the dynamical critical exponent $z \approx 1$.

$G_\theta(\mathbf{x} \to \infty, \tau \to \infty) \to M^2$ while $G_\theta(\mathbf{x} \to \infty, \tau = 0) \to M_{2D}^2$.

III. PHASE DIAGRAM FOR $\alpha = 0$

The phase diagram with $\alpha = 0$, determined from the calculations described below, is drawn with two different choice of axes, in Fig. 1. Part (b) of this figure is more revealing of the crossovers from finite temperatures to $T \to 0$ and of the effects of anisotropy in the temporal and spatial correlation lengths. The limit of $K_\tau \to 0$ is nonanalytic, with a crossover line separating a 2+1 D ordered phase from a region of pronounced correlations of the 2 D quasiordered

phase of the Kosterlitz-Thouless type with temporal disorder starting from the origin in Fig. 1(b). The line between the two phases represents the growing correlation of warps (instantons of monopoles-antimonopoles with total charge 0 [19], fully discussed in paper I) in the temporal direction. It shows, as expected, that a phase with 2D quasiorder exists for $1/E_c \lesssim N_\tau T$, (with a finite N_τ) where quantum effects are unimportant. The line ends for $1/(KK_\tau) \approx 7$ separating the disordered region from the (2+1)D ordered region.

The similarity of the phase diagram Fig. 1(a) in the K-K_τ plane to that in the K-α plane for fixed K_τ, given in Fig. 2 of paper I, is illustrative of the fact that reduced kinetic energy promotes a transition to the ordered phase, just as increasing
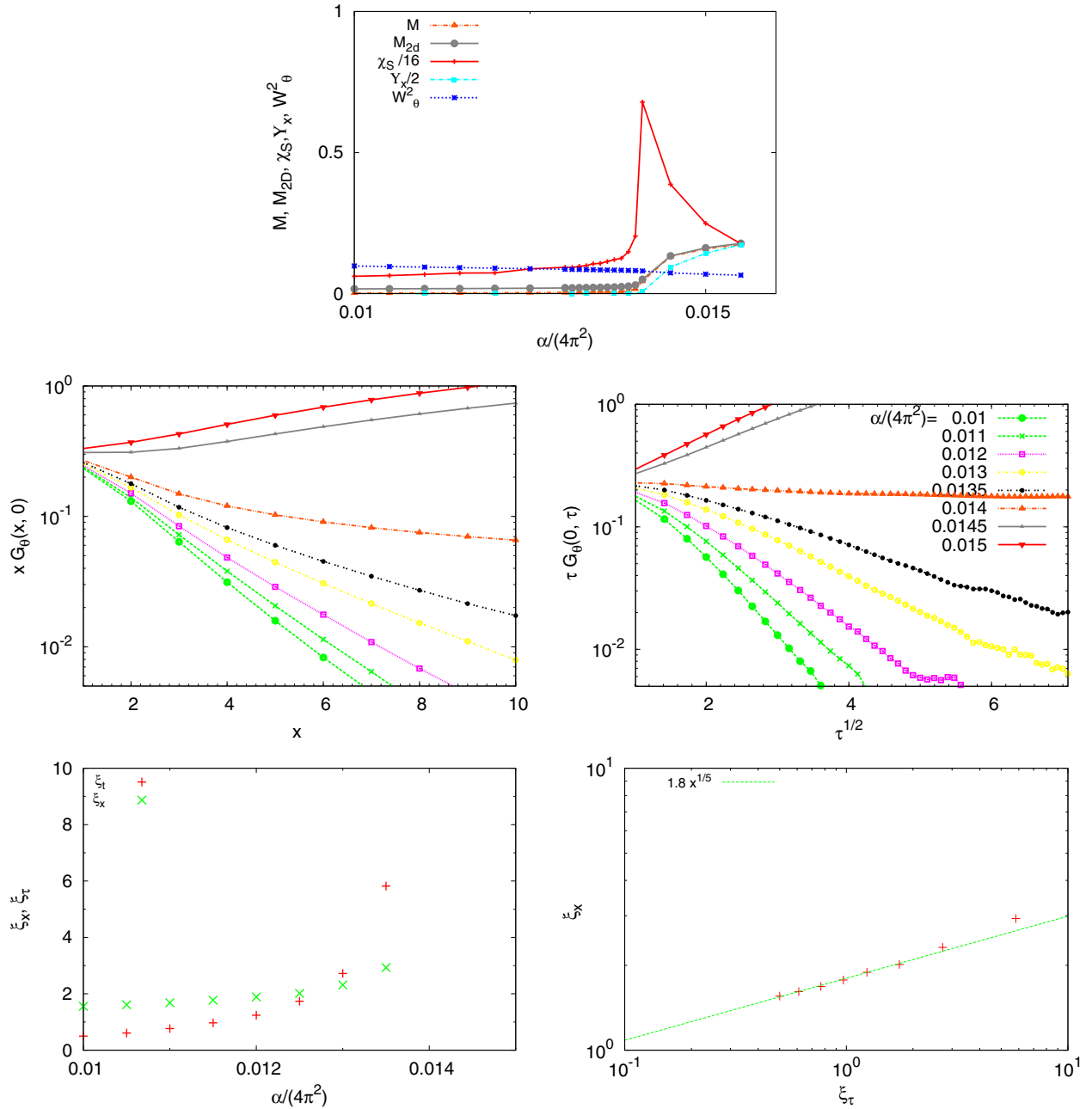
FIG. 6. This figure shows the same quantities and in the same order as in Figs. 4 and 5 but with $K_\tau = 0.15$, $K = 0.4$, and α is varied. A transition from disordered phase to ordered phase is observed above a critical α, as obvious from the static quantities on the top-most panel, and consistent with the correlation functions shown in the next pair of panels. But in contrast to the results in the two preceding figures for small α, if we fit the relation between correlation length and correlation time by a power law, we find $\xi_x \sim \xi_\tau^{1/z}$, with $z \approx 6$. The relation $\xi_x \sim \ln \xi_\tau$ yields an equally good fit in the range shown, consistent with $z \to \infty$.

dissipation does. For $\alpha = 0$ and $T = 0$, there is only one dimensionless parameter, which determines the condition for the 2+1 D transition. The purely 2D phase (the quasiordered or Kosterlitz-Thouless phase) exists only at finite T but crossovers to it is exhibited at $T \to 0$, as demarcated by the green line in Fig. 1(a). The situation changes when $\alpha \neq 0$, where we found in paper I that, within the accuracy of Monte Carlo determination of the helicity modulus Υ_x, 2D order parameter M_{2D} and (2+1)D order parameter M, a Kosterlitz-Thouless type transition occurs even for $T \to 0$, while the temporal correlations do not change.

We show now results of some of the calculations leading to the phase diagrams in Fig. 1. Figure 2 shows an example of the disordered to quasiordered 2D transition with $\alpha = 0$, $K_\tau = 0.1$ by varying K. Various static properties are plotted. The action susceptibility χ_S develops a peak at $K \approx 0.85$. Around this point, the 2D spatial order parameter M_{2d} as well as the helicity modulus Υ_x show a rapid growth and remain nonzero for further increase in K. The mean-square temporal fluctuation in angles, W_θ^2 hardly changes showing that there is no growth of correlations in the time direction. M is nonzero but nonmonotonic for $K \gtrsim 0.85$ for the calculation
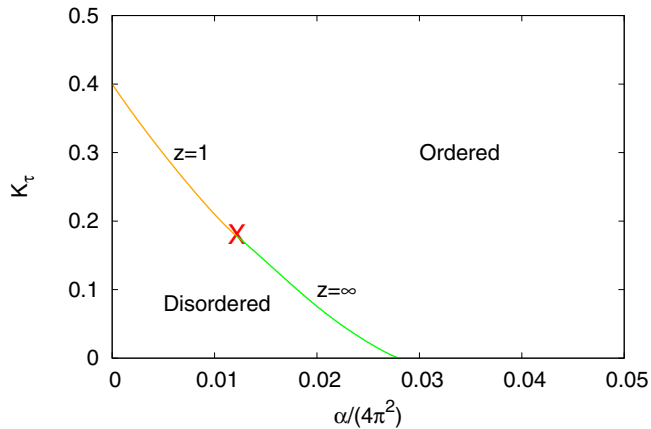
FIG. 7. Phase diagram in α-K_τ plane when $K = 0.4$. The red X marks the position where the transition changes from $z = 1$ 3DXY university class to $z = \infty$ local critical type. Such calculations have also been done for other values of K to demarcate the transition between $z = 1$ and $z = \infty$ criticality shown in the phase diagram in Fig. 8.

shown which has $N_\tau = 100$ but we have obtained results showing that M decreases for larger N_τ, and is consistent with being 0 asymptotically. It is difficult to study this behavior systematically as it shows large fluctuations. The results are consistent with what one expects of the quasiordered phase with spatial order (in each time slice) as evidence by the M_{2d} in Fig. 2, but disordered along the time direction. This is further corroborated by the study of the correlation functions.

Figure 3 shows results with $\alpha = 0$, $K = 1.4$ while K_τ is varied. Increasing K_τ drives the quasiordered 2D phase to the (2+1)D ordered phase. When $K_\tau \gtrsim 0.18$, $M \approx M_{2D}$, and $W_\theta^2 \to 0$ showing rapidly diminishing temporal fluctuations. The purely spatial characteristics such as M_{2D} and Υ_x increase only slightly. These results indicate the trend to order in the time direction, given that spatial order has already been achieved. We notice that χ_S has only a broad peak. This is due to the fact that, given a finite N_τ, we see a 2D to (2+1) D crossover rather than a transition, as mentioned earlier. We have checked and found that χ_S sharpens as a function of K_τ or larger N_τ.

We study the direct transition from the disordered phase to ordered phase, by choosing $K_\tau = 0.3$ and varying K. The various panels in Fig. 4 show a compendium of results, including the order parameter correlation functions and the relation of the spatial and the temporal correlation lengths. Both spatial and temporal ordering develop at a critical value K_c between 0.45 and 0.5. The spatial and temporal correlations show similar asymptotic behaviors near the critical point, $\propto \exp(-s/\xi_s)$, where $s = x$ or t. We find $\xi_x \sim \xi_\tau$ near the transition. This indicates, as expected for $\alpha = 0$, that the quantum transition has a dynamic critical exponent $z = 1$, i.e., it belongs to the classical 3d XY universality class.

IV. COMPLETE PHASE DIAGRAM

We recall the phase diagram calculated earlier in the K-α plane [1,2] in which K_τ was kept fixed at a few low values. The phase diagram appears similar to Fig. 1(a) with α replacing K_τ.
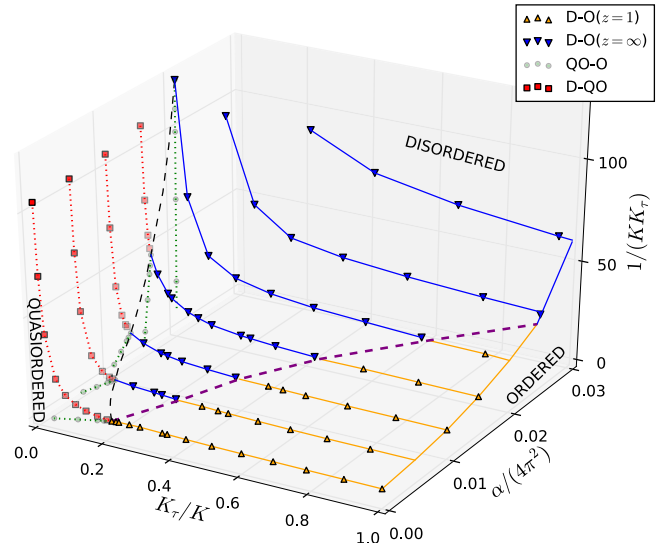

FIG. 8. The phase diagram in K_τ/K-α-$1/(K_\tau K)$ space. The parameter space for the disordered, ordered, and quasiordered states are specified. Purple dots show the disordered-ordered transition in $z = 1$ class while blue dots represent the same transition in $z \to \infty$ class. The transitions or crossovers between the quasiordered to ordered (green) and quasiordered to disordered (red) are also shown.

However, in the K-α plane, the 2D quasiordered phase appears via a true Kosterlitz-Thouless transition as verified in paper I by the size dependence of the helicity modulus at the transition as well as by the correlation function of the order parameter.

We have extended these calculations to other values of K and K_τ and α, which are necessary to discover the change from $z = 1$ to $z \to \infty$ in the phase diagram. A compendium of results from some of the new calculations are shown in the various panels of Figs. 5–7. We show the static quantities, M, M_{2D}, and Υ_x for various values of the parameters, as well as the order parameter correlations, $G(x,\tau)$ for fixed time as a function of x and for fixed x as a function of τ. From the correlation functions, the spatial correlation length ξ_x and the temporal correlation length ξ_τ and the relation between them are deduced.

From the results in these figures as well as calculations with other parameters, we deduce the set of transition lines (and crossovers) between the three different phases in the $1/(KK_\tau)$-α-K_τ/K space in Fig. 8. We find that the common point of the three phases in the $1/(K_\tau K)$-α plane changes for a fixed value of $K = 0.4$ from $1/KK_\tau \approx 12$ for $\alpha/4\pi^2 \approx 0.01$, $1/KK_\tau \approx 25$ for $\alpha/4\pi^2 \approx 0.018$ and for $1/KK_\tau \approx 250$ for $\alpha/4\pi^2 \approx 0.026$.

There is only one transition, from the disordered to the (2+1)D ordered phase, for $K_\tau \gtrsim K$ and $1/KK_\tau \lesssim 10$. A plot of ξ_x against ξ_τ is also shown, from which we find that this transition changes from one with $z = 1$ to that consistent with $z \to \infty$ for $\alpha/4\pi^2 \gtrsim 0.01$.

The change of z in the K_τ-α plane for a fixed value of K is shown in Fig. 7. At the small value, $K = 0.4$ for which the results are shown, there is no 2D quasiordered phase. The transitions occur, from the disordered phase when both K_τ and α are small, to the ordered phase for larger values of these parameters. However, depending on whether the critical value of K_τ
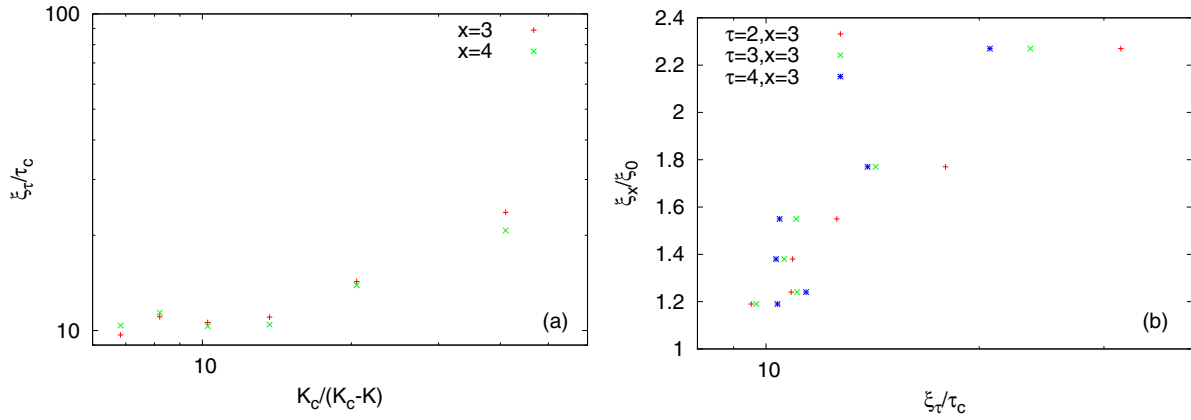
FIG. 9. Correlation lengths for transition driven by variation in the ratio of potential energy to kinetic energy, $K K_\tau$, for fixed dissipation. (a) The temporal correlation length ξ_τ as a function of $(K_c - K)$ for a fixed value of K_τ. Similar results are obtained as a function of K_τ for a fixed K. The critical value of the product $K K_\tau$ systematically decreases as the dissipation parameter α increases, as shown in the phase diagram of Fig. 8. (b) The spatial correlation length ξ_x increases very slowly as a function of $(K_c - K)$ compared to the temporal correlation length ξ_τ. We draw ξ_x on a linear scale and ξ_τ on a logarithmic scale to show that their relation appears consistent with $\xi_x \propto \ln \xi_\tau$.

is smaller than or larger than about 0.18, the transition has $z = 1$ or $z \to \infty$. We have evidence that the change occurs abruptly rather than smoothly. We show, in Figs. 6 and 5, the details of these two types of transitions, by two examples with K_τ fixed at 0.15, and 0.2 while α is varied. Similar results are also obtained for varying K_τ with fixed α. We also conclude from these and other results that the transition from the disordered to the ordered phase remains in the $z = 1$ class for $1/(K K_\tau) \lesssim 12$ for any value of α. This may be significant in relation to some of the experiments in superconductor-insulator transitions, in which $z = 1$ and $\nu = 2/3$ has been deduced [4,20]. One should note however that exponents varying from these are also obtained in different samples. We would suggest deducing the systematics of $K K_\tau$ in experiments as samples are varied.

V. CORRELATION FUNCTIONS AT THE DISORDERED TO ORDERED TRANSITION AS A FUNCTION OF $(K K_\tau)$

In paper I, we studied the correlation function at the disordered to (2+1)D ordered transition as a function of the dissipation parameter α for fixed K and K_τ. We provide results in Fig. 9 for the order parameter correlation function when the transition at large fixed α is driven by increasing the product $\overline{K}^2 \equiv (K K_\tau)$. We recall that as a function of the deviation of the dissipation parameter α from its critical value α_c for fixed K and K_τ, ξ_τ has an essential singularity, and the spatial correlation length is consistent with varying as the logarithm of the temporal correlation length, i.e., $z \to \infty$. On the other hand, we find that for fixed α and K_τ, the behavior
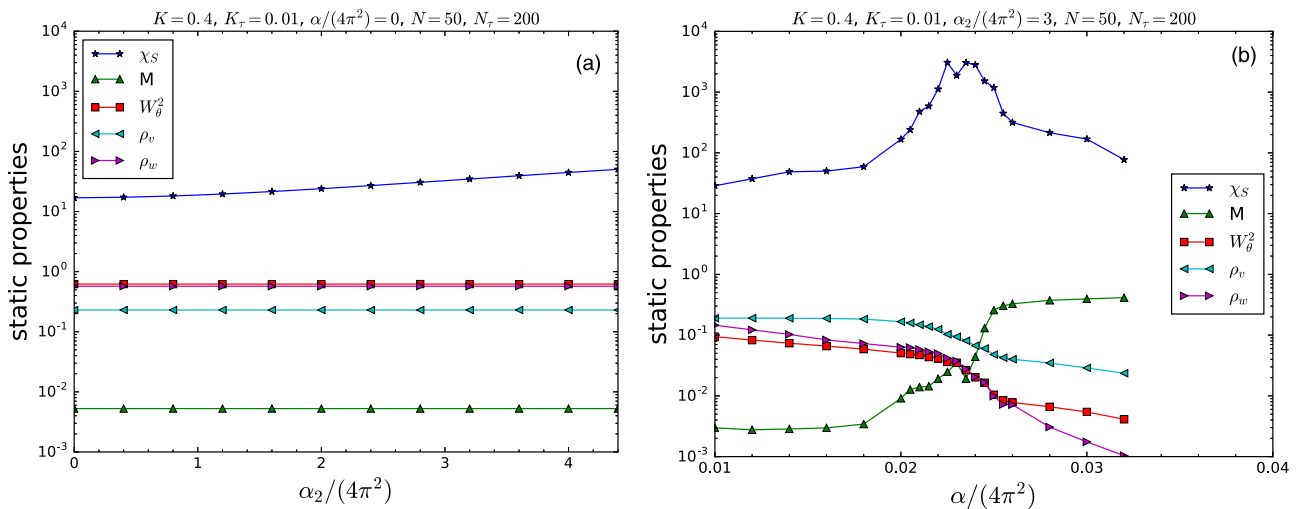

FIG. 10. (a) Static quantities calculated for varying values of the parameter α_2 for the periodic form of dissipation, with the parameter α for Caldeira-Legett form of dissipation kept at 0. This calculations (and a few others not shown) are in the range below the critical $K K_\tau$ in which there is a transition for $\alpha_2 = 0$. In this range, it is shown that there is no transition caused by increasing α_2. (b) Static quantities calculated for a large fixed value of α_2 as a function of α. Comparison with the same quantities calculated in Fig. 6 of paper I for $\alpha_2 = 0$ shows that a finite value of the latter has no observable consequences for the nature of the transition.

as a function of K is

$$\xi_\tau/\tau_c = \left(\frac{K_c - K}{K_c}\right)^{-\nu_\tau}, \qquad (9)$$

with $\nu_\tau \approx 0.5$. However, as also shown in Fig. 9, the very slow variation of ξ_x compared to ξ_τ, consistent with $\xi_x/a \propto \ln(\xi_\tau/\tau_c)$ continues to hold. Similar exponent is found for variation of K_τ for fixed α and K. The calculation show that the critical $\overline{K}_c = \sqrt{KK_{\tau c}}$ continuously decreases towards 0 as α becomes larger and larger. This is also exhibited in Fig. 8.

In experimental systems, ranging from the ferromagnetic to antiferromagnetic and loop-order quantum criticality, the variation of the parameter (KK_τ) is more likely to drive the transition rather than the dissipation parameter α. The superconductor-insulator transitions may be driven by either parameter. The result that a transition can occur for smaller values of $\sqrt{KK_\tau}$ as α increases is a very important verifiable prediction for experiments.

VI. DISORDER TO ORDER TRANSITION FOR DIFFERENT FORMS OF DISSIPATION

We have presented calculations above and in paper I with the Caldeira-Leggett form of dissipation—the third term in the action, Eq. (1). This form of dissipation is clearly allowed even though it does not preserve the periodicity $\theta(\mathbf{x}, \tau) \to \theta(\mathbf{x}, \tau) + 2\pi$. It represents the coupling of the collective mode current, proportional to $\nabla\theta$, to fermion currents in the metallic models of interest. Another form of allowed dissipation preserves periodicity:

$$S_{2,\text{diss}} = \frac{\alpha_2}{4\pi^2} \sum_{\langle \mathbf{x}, \mathbf{x}' \rangle} \int d\tau d\tau'$$

$$\times \frac{\pi^2}{\beta^2} \frac{\cos((\theta_{\mathbf{x},\tau} - \theta_{\mathbf{x}',\tau}) - (\theta_{\mathbf{x},\tau'} - \theta_{\mathbf{x}',\tau'}))}{\sin^2\left(\frac{\pi|\tau - \tau'|}{\beta}\right)}. \qquad (10)$$

Calculations with, in effect, periodic dissipation alone have been presented earlier [15]. The result is that the transition with and without such a dissipation remains in the same class, i.e., with $z = 1$. We present in Fig. 10 calculations with both forms of dissipation present and for for kinetic and potential energy parameters fixed so that the transition studied is from the disordered state to the fully ordered state in the range in which increasing α leads to the transition in the $z \to \infty$ class. The two parts of Fig. 10 are (a) varying α_2 for fixed $\alpha = 0$. We have found that these results remain unchanged for α less than about the critical value in the absence of α_2. (b) With fixed large α_2 varying α across the critical value α_c for $\alpha_2 = 0$. On comparison with results presented in Fig. 6 of paper I, the conclusion from (a) is that there is no transition as a function of α_2 for a very wide range of its variation for $\alpha = 0$. The conclusion from (b) is that all the quantities calculated have precisely the same form on either side of the transition as a function of α as in the calculation with $\alpha_2 = 0$. In fact, even the location of the transition as a function of α does not appear to change.

Together with earlier results [15], the conclusion is that for small enough α, the disorder to $(2+1)$D order transition as a function of KK_τ, for any reasonable value of the periodic dissipation α_2, retains the $z = 1$ class as for $\alpha_2 = 0$. On the other hand, $\alpha_2 \neq 0$ does not affect the transition for the range of KK_τ in which it is driven by increasing the Caldeira-Leggett dissipation α.

[1] L. Zhu, Y. Chen, and C. M. Varma, Phys. Rev. B **91**, 205129 (2015).

[2] E. B. Stiansen, I. B. Sperstad, and A. Sudbø, Phys. Rev. B **85**, 224531 (2012).

[3] S. Chakravarty, G.-L. Ingold, S. Kivelson, and G. Zimanyi, Phys. Rev. B **37**, 3283 (1988).

[4] Y.-H. Lin, J. Nelson, and A. Goldman, Physica C **514**, 130 (2015).

[5] C. M. Varma, Phys. Rev. Lett. **115**, 186405 (2015).

[6] C. M. Varma, Rep. Prog. Phys. **79**, 082501 (2016).

[7] M. E. Simon and C. M. Varma, Phys. Rev. Lett. **89**, 247003 (2002).

[8] P. Bourges and Y. Sidis, C. R. Phys. **12**, 461 (2011).

[9] H. Löhneysen, A. Rosch, M. Vojta, and P. Wölfle, Rev. Mod. Phys. **79**, 1015 (2007).

[10] C. Hou and C. M. Varma, Phys. Rev. B **94**, 201101(R) (2016).

[11] S. Doniach, Phys. Rev. B **24**, 5063 (1981).

[12] M. P. A. Fisher, Phys. Rev. Lett. **57**, 885 (1986).

[13] K.-H. Wagenblast, A. van Otterlo, G. Schön, and G. Zimányi, Phys. Rev. Lett. **79**, 2730 (1997).

[14] A. Caldeira and A. Leggett, Ann. Phys. (NY) **149**, 374 (1983).

[15] I. B. Sperstad, E. B. Stiansen, and A. Sudbø, Phys. Rev. B **84**, 180503 (2011).

[16] J. V. José, L. P. Kadanoff, S. Kirkpatrick, and D. R. Nelson, Phys. Rev. B **16**, 1217 (1977).

[17] V. Aji and C. M. Varma, Phys. Rev. Lett. **99**, 067003 (2007).

[18] V. Aji and C. M. Varma, Phys. Rev. B **79**, 184501 (2009).

[19] V. Aji and C. M. Varma, Phys. Rev. B **82**, 174501 (2010).

[20] M. A. Steiner, N. P. Breznay, and A. Kapitulnik, Phys. Rev. B **77**, 212501 (2008).